Numerical Modeling of Dispersed Particle Motion in Pipelines with Abrupt Contractions

Abdulfatto Ibrokhimov [1, 2, a)] , Akmal Mirzoev [3, b)] and Ilkhom Akhmadov [4, c)]

[1] *Fergana state technical university, Fergana, Uzbekistan,*
[2] *Belarus–Uzbekistan Intersectoral Institute of Applied Technical Qualifications Tashkent, Tashkent, Uzbekistan Tashkent,*
[3] *Institute of Mechanics and Seismic Stability of Structures named after M.T.Urazbaev, Uzbekistan Academy of Sciences, 100125, Tashkent, Dormon yuli, 40, Uzbekistan.*
[4] *Navoi state university, Navoi, Uzbekistan.*

[a)] Corresponding author: Ibroximov-2022@mail.ru
[b)] akmal.mirzoev78@mail.ru
[c)] Ilhomahmadov0516@gmail.com

Abstract. In this study, the numerical modeling of dispersed particle transport and fluid flow through a sudden contraction, where a larger-diameter pipe transitions into a smaller-diameter pipe, was carried out. To capture the turbulent characteristics of the carrier fluid, the Spalart–Allmaras (SA) turbulence model was employed due to its proven efficiency in predicting boundary-layer flows and separation phenomena in engineering applications. For the dispersed phase, the Volume of Fluid (VOF) approach was applied to accurately track the particle trajectories and their interaction with the continuous phase. This combination of turbulence modeling and multiphase treatment allowed a detailed investigation of the flow structure, particle behavior, and dispersion mechanisms in the contraction zone. The numerical simulations provided insights into the velocity distribution, turbulence intensity, and particle concentration under varying flow conditions, offering a deeper understanding of multiphase flow dynamics in geometries with sudden area changes.

INTRODUCTION

The mathematical modeling of multiphase fluid dynamics remains a highly intricate task, as the conventional Navier–Stokes equations alone cannot fully describe such systems. In addition to the equations governing the continuous carrier phase, it is necessary to introduce complementary formulations that capture the dynamics of the dispersed phase, along with momentum exchange terms that represent interfacial fluid–particle interactions.

Several modeling strategies have been developed in this regard. The Lagrangian description, often realized through the Discrete Phase Model (DPM), treats particles as discrete entities whose individual trajectories are explicitly tracked within the flow field. In contrast, the Eulerian framework considers particle motion in terms of averaged field variables—such as velocity, pressure, and concentration—yielding a continuum representation of the dispersed phase. Another widely employed methodology is the Volume of Fluid (VOF) approach, which is particularly suited for resolving immiscible multiphase interfaces, as it allows for accurate reconstruction of phase boundaries and captures interface dynamics under transient flow conditions.

Together, these approaches—DPM, Eulerian formulations, and VOF—offer complementary perspectives and are frequently combined in hybrid strategies to enhance predictive capability in complex multiphase flow simulations. [1-5]:

The formulation of mathematical models for two-phase turbulent flows represents one of the most challenging tasks in modern hydrodynamics. Approaches such as Direct Numerical Simulation (DNS) and Large Eddy Simulation (LES) demand substantial computational resources, and their application to complex aerodynamic problems is feasible only with the use of high-performance computing systems [1].

Turbulence anisotropy occurs, for example, in flows where flow recirculation is observed. Flow recirculation is one of the main ways to increase mixing of solid particles. Nevertheless, these results are very important in practice for designing various pipelines [4]. However, the development of modern science and technology requires more accurate calculation results, which requires the development of more adequate turbulence models.

Systems for providing the necessary climatic conditions in working, residential and other premises are integral technological elements of modern buildings, and they account for a significant portion of capital investments and operating costs [5-8]. Knowledge of the fundamentals of modeling and optimizing flow distribution in such utility networks allows planning and implementing measures aimed at resource conservation, environmental protection and improving the efficiency of equipment.

The main element of the engineering communication networks are pipelines and liquids or gases flowing through them at a certain speed. From a hydrodynamic point of view, liquid or gas flows have different natures: laminar, transitional, and three turbulent subregimes [9-12,1]. Reliable phenomenological results of isothermal flow are available only for the laminar flow regime. In other flow regimes, engineering calculations are based on semi-empirical dependencies. The quasi-one-dimensional approach used in flow modeling is heuristic in nature and allows obtaining formulas acceptable for engineering practice [5-7, 11,].

In mathematical modeling of quasi-one-dimensional isothermal flow, the laws of conservation of mass and momentum are taken into account. According to the latter law, a change in pressure is expressed by three internal forces: the local and convective components of the inertial force of the medium and the friction force, and the external force, which is caused by the force of gravity [8, 9, 12]. Depending on the share of gravitational force in the heat and mass transfer process, three different energy flow regimes are expected [3]. At positive and zero slope of the route, as well as at small negative slopes, a path decrease in pressure is observed. At a certain negative (critical) slope of the section, the pressure along the length can remain constant, which is explained by the balance of the friction force and the change in the potential energy of the fluid, caused by the gravitational force. At smaller values of the slope than the critical, a path increase in pressure is observed. This regime is called "post-peri-valley" and the presence of such a regime in main gas pipelines is proven in [20].

The isothermal approximation in modeling the pipeline process of transporting liquids, gases and other mixtures works under certain conditions, for example, if the pipeline is short, the speed is low, the intensity of heat exchange with the environment is insignificant. In other cases, heat exchange with the environment should be taken into account.

PHYSICAL FORMULATION OF THE PROBLEM

The transport of solid particles by a natural flow is, in its physical essence, analogous to the hydraulic transport of soils and rocks eroded by water; therefore, the problems of hydraulic transport and the dynamics of suspended natural flow are very similar. However, due to differing objectives, these problems are considered separately, although they share a common theoretical and physical basis.

The length of the large pipe is 100 mm, the small pipe is 50 mm, and the total pipe length is 800 mm.

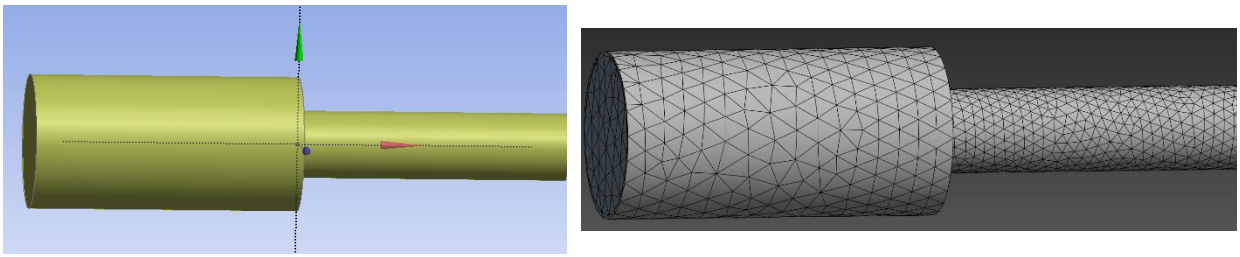

a) b)

FIGURE 1. Geometry of the pipe with a convex insert and the calculation grid

MATHEMATICAL FORMULATION OF THE PROBLEM

For the numerical study of this problem, the system of Reynolds-averaged Navier-Stokes equations is used, which takes into account the interaction between the phases [11]. The system of equations does not take into account the forces arising from turbulent migration, Sefman, Magnus (lift force) and the Coriolis effect [12]. Because they are much less than gravity. Thus, for mathematical modeling of the processes of transfer of air bubbles, precipitation and

aerosols into the channels, it is sufficient to take into account the force of gravity and the Stokes force of phase interaction.

$$\begin{cases} \dfrac{\partial \overline{U}_j}{\partial x_j} = 0 \\ \dfrac{\partial \overline{U}_i}{\partial t} + U_j \dfrac{\partial \overline{U}_i}{\partial x_j} = -\dfrac{1}{\rho}\dfrac{\partial P}{\partial x_i} + \dfrac{\partial}{\partial x_j}\left[\nu\left(\dfrac{\partial \overline{U}_i}{\partial x_j} + \dfrac{\partial \overline{U}_i}{\partial x_j}\right)\right] + \dfrac{1}{\rho}\dfrac{\partial}{\partial x_j}\left(-\rho\overline{u_i' u_j'}\right) - \sum_{m=1}^{N}\dfrac{\rho_m}{\rho}k_m\left(\overline{U}_i - \overline{U}_{p_i}\right) \\ \dfrac{\partial \overline{U}_{p_i}}{\partial t} + \overline{U}_j \dfrac{\partial \overline{U}_{p_i}}{\partial x_j} = k_m\left(\overline{U}_i - \overline{U}_{p_i}\right) \\ \dfrac{\partial \rho_m}{\partial t} + \overline{U}_{p_i}\dfrac{\partial \rho_m}{\partial x_j} = D\dfrac{\partial}{\partial x_j}\left[\dfrac{\partial \rho_m}{\partial x_j} + \dfrac{\partial \rho_m}{\partial x_i}\right] \end{cases} \tag{11}$$

Here $\overline{U}_i$ – longitudinal and transverse of the fluid flow velocity; $\overline{U}_{pi}$ - similar velocity components for m-th particle fractions; p – hydrostatic pressure; ρ – density of fluid; ν, ν_t - molecular and turbulent viscosities; ρ_m - particle mass density; m- number of particle fractions; $D = \dfrac{\rho}{Sc\,(\rho + \rho_p)}(\nu + \nu_t)$ is the diffusion coefficient for the precipitate phase, $Sc = 0.8$ is the Schmidt coefficient.

The interaction coefficient between the phases was determined by the Stokes parameter:

$$k_m = \frac{18\rho\nu}{\rho_p \delta_m^2}, \tag{2}$$

In this expression, ρ_p the density of the deposits δ_m is the diameter of the deposits.

The system of Navier-Stokes equations averaged over Reynolds (1) is not closed. To close this system in linear models, the generalized Boussinesq hypothesis [10] is used.

$$u_i' u' = \nu_t\left(\frac{\partial \overline{U}_i}{\partial x_j} + \frac{\partial \overline{U}_i}{\partial x_j}\right) - \frac{2}{3}k\delta_{ij} \tag{3}$$

Here ν_t is turbulent viscosity.

The thesis used the highly acclaimed Spalart-Allmares model. The differential form of this model is as follows [11]:

$$\begin{aligned} \frac{\partial \widetilde{\nu}}{\partial t} + U_j\frac{\partial \widetilde{\nu}}{\partial x_j} = C_b\left(1 - f_{t,2}\right)\widetilde{S}\,\widetilde{\nu} - \left[C_{w1}f_w - \frac{C_{b1}}{k^2}f_{t2}\right]\left(\frac{\widetilde{\nu}}{d}\right)^2 + \\ + \frac{1}{\sigma}\left[\left(\frac{\partial}{\partial x_j}\left(\nu + \widetilde{\nu}\right)\frac{\partial \widetilde{\nu}}{\partial x_j}\right) + C_{b2}\frac{\partial \widetilde{\nu}}{\partial x_i}\frac{\partial \widetilde{\nu}}{\partial x_i}\right] \end{aligned}, \tag{4}$$

The turbulent viscosity coefficient is defined as:

$$\nu_t = \widetilde{\nu} f_{v1}, \tag{5}$$

Additional features and parameters of the model are as follows:

$$f_{v1} = \frac{x^3}{x^3 + c_{v1}^3}, \quad x = \frac{\widetilde{\nu}}{\nu}, \quad \widetilde{S} = \Omega + \frac{\widetilde{\nu}}{k^2 d^2}f_{v2}, \quad \Omega = \sqrt{W_{ij}W_{ij}}, \tag{6}$$

$$f_w = g\left[\frac{1+C_{w3}^6}{g^6+C_{w3}^6}\right],\ g = r + C_{w2}\left(r^6 - r\right),$$
$$f_{v2} = 1 - \frac{x}{1+xf_{v1}},\ g = r + C_{w2}\left(r^6 - r\right),$$
$$f_{t2} = c_{t3}\exp\left(-c_{t4}x^2\right),\ r = \min\left[\frac{\tilde{\nu}}{\tilde{S}k^2d^2}, 10\right] \quad (7)$$
$$W_{ij} = \left(\frac{1}{2}\frac{\partial U_i}{\partial x_j} - \frac{\partial U_j}{\partial x_i}\right)$$

Here, Ω - is the vortex size, S - is the strain rate, d -is the nearest distance to the wall

TABLE.1. Model constants

σ_v	k_r	C_{b1}	C_{b2}	C_{v1}	C_{w1}	C_{w2}	C_{w3}	C_{r1}	C_{r2}	C_{r3}
2/3	0.41	0.1335	0.622	7.1	$C_{w1} = \frac{C_{b1}}{k^2} + \frac{1+C_{b2}}{\sigma}$	0.3	2.0	1	12	1

ANALYSIS OF NUMERICAL RESULTS.

In the numerical simulations, the Spalart–Allmaras (SA) turbulence model was employed to capture the effects of turbulence in the converging pipe flow. The computational domain was discretized using a structured/unstructured mesh with local refinement near the pipe wall to accurately resolve the boundary layer. Grid independence tests were performed to ensure that the numerical results were not sensitive to the mesh density.

The governing equations were solved in ANSYS Fluent using the finite volume method. Pressure–velocity coupling was handled through the SIMPLE algorithm, while second-order spatial discretization schemes were applied for momentum and turbulence equations to improve accuracy. Convergence was monitored by tracking the scaled residuals and key flow parameters until steady and repeatable solutions were achieve

On fig. 2 we compare the numerical results with the experimental ones, where the flow has passed into a completely turbulent state and reached a constant value. Here U is the fluid velocity at the inlet.

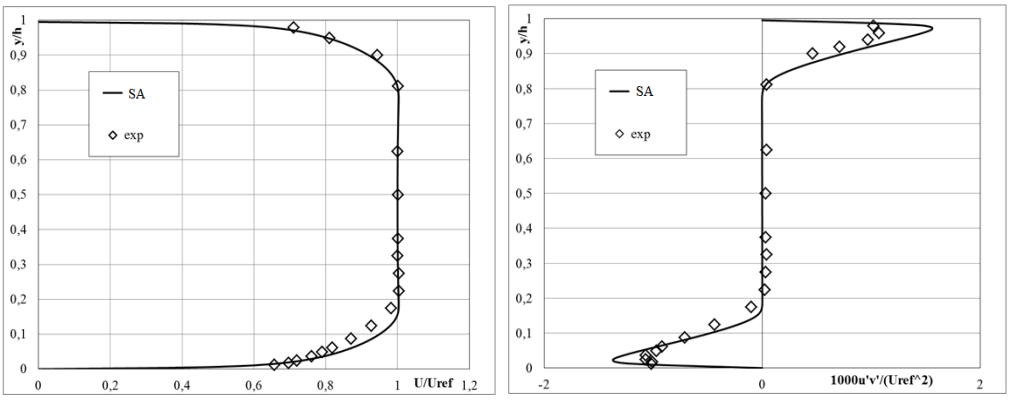

a) b)

FIGURE 2. Comparison of numerical results with experimental data: [5] a) longitudinal velocity U, b) Reynolds stresses u'v'.

On fig. 3 shows the dependence of the friction coefficient of the pipe on the thickness of the momentum loss. The results of this experiment were taken from Karman [2].

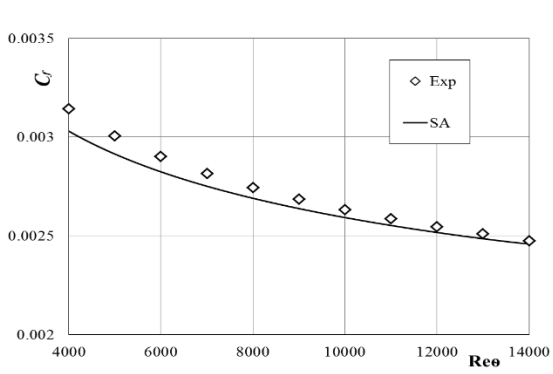

FIGURE 3. Dependence of the coefficient of friction on the Reynolds number of the momentum loss thickness.

Figure 4 presents the streamline distribution, which demonstrates a pronounced rise in velocity within the contracted section of the pipe. This behavior is associated with the reduction in cross-sectional area, resulting in the acceleration of the flow

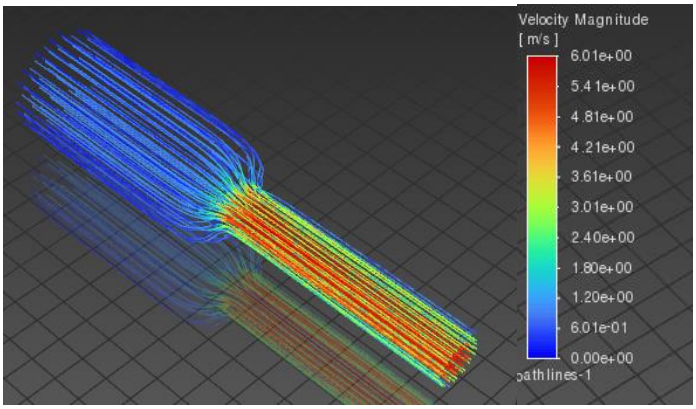

FIGURE 4. The streamlines are depicted.

In Figure 5, the particle motion at different concentrations and their settling at various times are depicted in 3D. At the location where the pipe diameter changes, both the fluid velocity and the particle velocity varied significantly. In this case, the SA turbulence model provided a good representation of the process, while the VOF model was used for the particles.

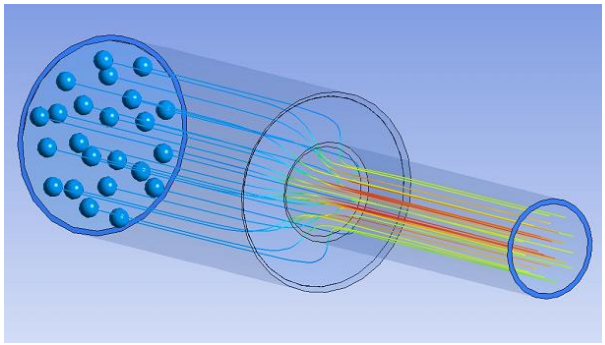

T=5 sek

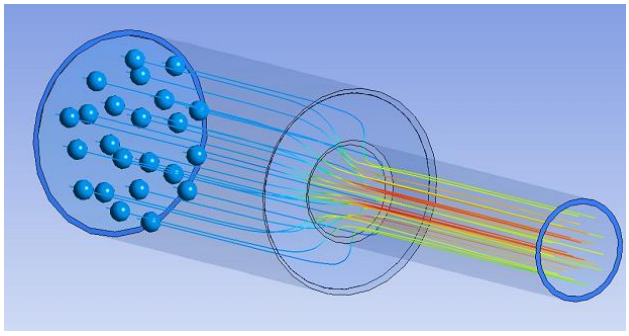

T=15 sek

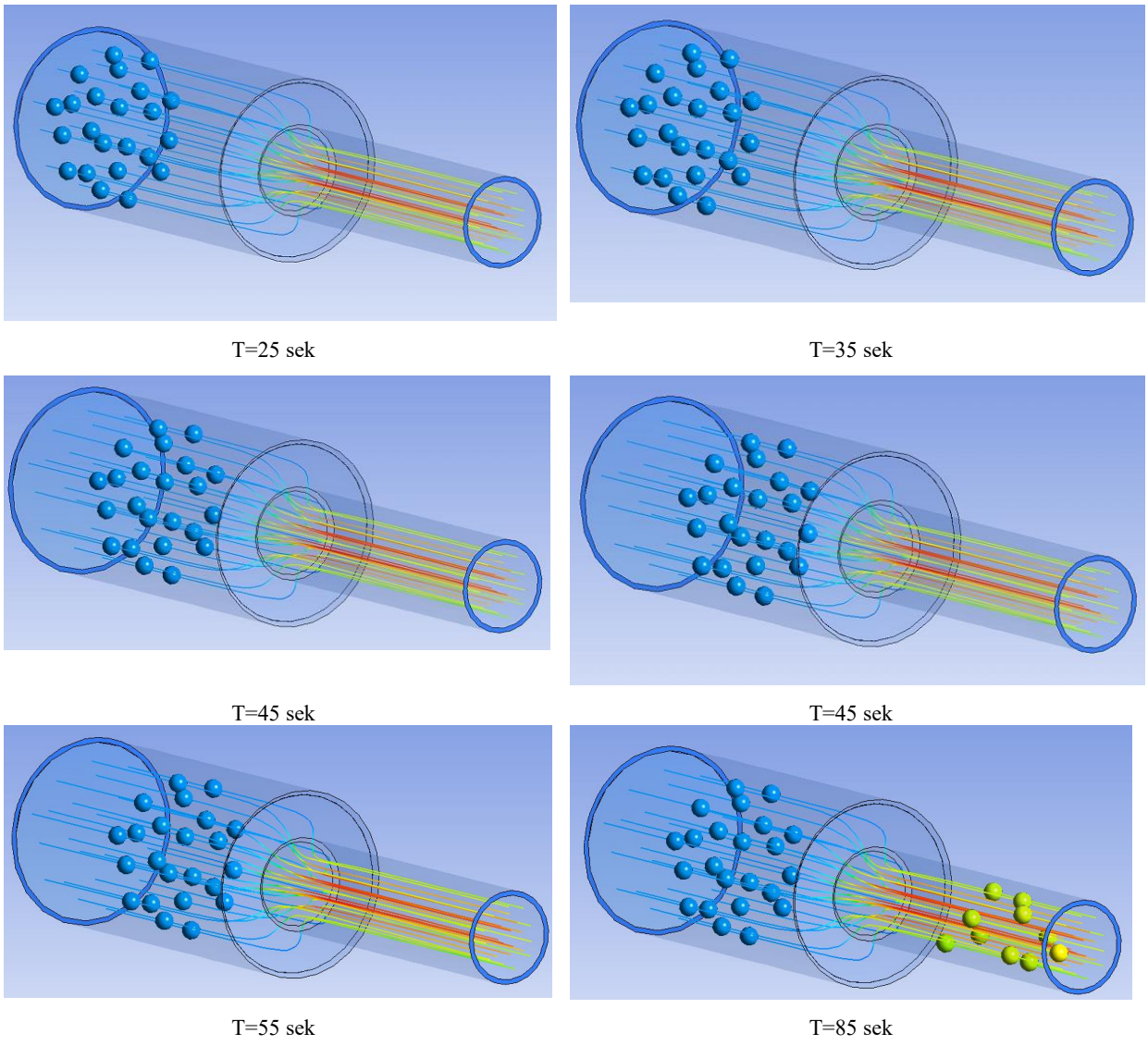

FIGURE 5. The trajectory of particles in a three-dimensional pipe

CONCLUSION

In this study, the flow of dispersed particles in a converging pipe was investigated numerically. The SA turbulence model was employed, and the results were compared with experimental data. The process was simulated using the modern ANSYS Fluent software. The particle trajectories were determined based on the VOF approach. The motion of particles at different time intervals was analyzed numerically.

ACKNOWLEDGMENTS

This study was made possible by budget funding from the Uzbekistan Academy of Sciences. We express our sincere gratitude to the Academy for its ongoing support and commitment to advancing scientific research.

REFERENCES

1. A. I. Ibrokhimov, M. E. Madaliev, R. A. Fayziyev and A. A. Mirzoev, “Numerical Simulation of Separate Flow Around a Heated Square Cylinder,” in *ICFNDS-2022,* edited by A. Aziz (ACM, Tashkent, 2022), pp.23-26.

2. M. A Shoyev, A. R. Ibroximov, M. E. Madaliev, O. Q. Rayimqulov and M. N. Ismatov, “Numerical study of modified centrifugal cyclone,” in *CONMECHYDRO-2023*, E3S Web of Conferences 401, edited by D. Bazarov (EDP Sciences, Tashkent, 2023), 01036.
3. A. Ibrokhimov, A. Mirzoev, S. Misirov, A. Matkarimov and K. Djumaev, “Comparison of the results of applying the turbulence model VT− 92 and two-fluid model to the problem of a subsonic axisymmetric jet,” in *IPFA-2023*, E3S Web of Conferences 452, edited by S. Yekimov *et al.* (EDP Sciences, Dnipro, 2023), 02026.
4. A. A. Mirzoev and Y. D. Khodjayev, International Journal of Innovative Technology and Exploring Engineering **8**, 3700-3704 (2019).
5. Z. Malikov, A. Mirzoev, M. Madaliev, D. Yakshibayev and A. Usmonov, “Numerical simulation of flow through an axisymmetric two-dimensional plane diffuser based on a new two-fluid turbulence model,” in *ICISCT- 2021*, edited by J. Brown (Red Hook, NY, 2021), pp.1-7.
6. Z. M. Malikov, A. A Mirzoev and M. Madaliev, Journal of Computational Applied Mechanics **53**, 282-296 (2022).
7. Z. Malikov, Applied Mathematical Modelling **104,** 34–49 (2020).
8. O. Otajonov and Z. Sattorov, “Strength characteristics of aerated concrete with fly ash filler from Angren Thermal Power Plant,” in *CONMECHYDRO-2023,* E3S Web of Conferences 365, edited by D. Bazarov (EDP Sciences, Tashkent, 2023), 01036.
9. Y. Zhang, L. Xiaobing, X. Zhang and L. Peng, Energies **13 (18),** 49-52 (2020).
10. Z.Malikov, Applied Mathematical Modeling **82**, 409-436(2022)
11. K. Navruzov and S. B. Sharipova, Fluid Dynamics 58, 360-370 (2023).
12. K. Navruzov, R. A. Fayziyev, and A. A. Mirzoev, “Tangential Shear Stress in an Oscillatory Flow of a Viscoelastic Fluid in a Flat Channel,” in NEW2AN-2022, edited by Y. Koucheryavy *et al*. (Springer, Tashkent, 2023), pp.1-14.